JCTC Journal of Chemical Theory and Computation

Article

pubs.acs.org/JCTC

Crystal Polymorphism in Oxalyl Dihydrazide: Is Empirical DFT-D Accurate Enough?

Shuhao Wen and Gregory J. O. Beran*

Department of Chemistry, University of California, Riverside, California 92521, United States

Supporting Information

ABSTRACT: Crystalline oxalyl dihydrazide has five experimentally known polymorphs whose energetics are governed by subtle balances between intra- and intermolecular interactions, providing a severe challenge for theoretical crystal structure modeling. Previous work has shown that many common density functional methods that neglect van der Waals dispersion cannot correctly describe this system, but it has been argued that empirically dispersion-corrected DFT-D performs much better. Here, we examine these crystals with second-order Møller−Plesset perturbation theory (MP2) and related levels of theory using the fragment-based hybrid many-body interaction method. The energetics prove sensitive to the treatment of electron−electron correlation, the basis set, many-body induction, three-body dispersion, and zero-point contributions. Nevertheless, our best predictions for the polymorph energy ordering based on dispersion-corrected MP2C calculations agree with the available experimental data. In contrast, lower levels of theory, including the common B3LYP-D* and D-PW91 dispersion-corrected density functional approximations, fail to reproduce experimental observations and/or the high-level calculations.

1. INTRODUCTION

The presence of multiple crystal packing motifs, or polymorphs, can have dramatic implications for pharmaceuticals, organic semiconductors, and many other chemical applications. Ideally, one would be able to predict and explain molecular crystal polymorph energetics theoretically, but such crystal structure prediction is extremely challenging. Accurate molecular crystal structure modeling requires computational chemistry techniques capable of discriminating energy differences that can be as small as 1 kJ/mol or less while describing a mixture of intramolecular and noncovalent intermolecular interactions (hydrogen bonding, electrostatics, and van der Waals dispersion) with uniform accuracy.

Despite the daunting challenges inherent to crystal structure prediction, the past several years have witnessed remarkable progress in several directions, all of which stem from the incorporation of quantum mechanical (QM) techniques into the crystal models. First, the quality of molecular mechanics (MM) force fields and QM-based force-field parametrization strategies have improved tremendously.[1,2] Second, the application of periodic density functional theory (DFT) to molecular crystal problems is rapidly becoming routine. DFT predictions are often quite good, as long as van der Waals dispersion interactions are included (usually, but not always,[3−9] with empirical corrections such as DFT-D[10]). The high rates of success in the two most recent blind tests of crystal structure prediction, for instance, reflect these two improvements.[11−15]

Despite the achievements of periodic DFT for molecular crystals, increasing evidence indicates that standard density functional approximations are not always sufficiently reliable for polymorph discrimination. For instance, empirical dispersion-corrected DFT fails to predict the virtual degeneracy of the two aspirin polymorphs. Instead, it overstabilizes form II by a couple of kilojoules per mole.[16] Even more concerning, the variations in the predictions between different, seemingly reasonable density functionals can be very large, sometimes exceeding the polymorphic energy differences in question. Such behavior has been seen in diiodobenzene,[17] glycine,[18,19] ortho-acetamidobenzamide,[20] and oxalyl dihydrazide.[20]

Oxalyl dihydrazide (Figure 1) is a particularly pathological case of conformational polymorphism in which the relative energies of the five experimentally known polymorphs[21] vary wildly with the choice of basis set and functional. The difficulty here stems from the need to balance the diverse mixtures of intramolecular hydrogen bonding, intermolecular hydrogen bonding, and intermolecular π-stacking van der Waals dispersion interactions in the five different structures.

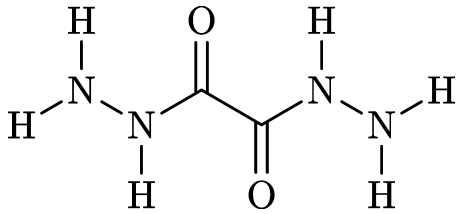

Figure 1. Oxalyl dihydrazide, $C_2H_6N_4O_2$.

As described in ref 21, the α polymorph involves purely intermolecular hydrogen bonding, and it is the most dense form (1.76 g/cm^3). The β, γ, δ, and ε polymorphs all involve mixtures of inter- and intramolecular hydrogen bonding and are less dense (1.59−1.66 g/cm^3). Experimental data on the relative stabilities is incomplete, but it is believed that α, δ, and ε polymorphs are the most stable, though the ordering among those three is unknown. All three undergo an endothermic phase transition to the γ form at high temperatures, suggesting

Received: June 11, 2012
Published: July 27, 2012

that γ is less stable than the other three. Finally, the difficult-to-produce, metastable β form is thought to be the least stable polymorph.

Earlier work using the dispersion-corrected D-PW91 functional did predict a plausible polymorph stability ordering.[20] However, as the authors noted, the polymorph energies spanned a range of more than 15 kJ/mol, which is 50% larger than the typically accepted 10 kJ/mol range[22] for experimentally observed polymorphs. Furthermore, as we will demonstrate here, another seemingly reasonable dispersion-corrected functional, B3LYP-D*,[23] makes completely different predictions. These results raise questions about the robustness of these dispersion-corrected DFT predictions in oxalyl dihydrazide.

Wave function-based electronic structure methods provide alternatives to DFT in such situations. Major advances in local correlation methods for periodic systems have made periodic MP2 feasible in molecular crystals, with impressive results.[24] However, the computational cost remains too high for many interesting systems.

More recently, fragment-based electronic structure methods have made it possible, for the first time, to go beyond periodic DFT to high-level *ab initio* wave function techniques in molecular crystals containing dozens or even hundreds of atoms per unit cell.[25] The key advantage of these fragment approaches lies in the ability to systematically improve the quality of the predictions. Demonstrating convergence of the calculated results with respect to the theoretical model chemistry is critical to making robust predictions regarding the small energy differences in molecular crystals. For instance, we explained the experimentally observed intergrowths of the two aspirin polymorphs by demonstrating that the two forms lie within a few tenths of a kilojoule per mole of each other and that this prediction is highly robust with respect to the user-chosen theoretical model chemistry.[16]

In this study, we use our fragment-based hybrid many-body interaction (HMBI) QM/MM model[26] to perform second-order Møller−Plesset perturbation theory-level (MP2) calculations on the five polymorphs of oxalyl dihydrazide. We also perform calculations with two dispersion-corrected MP2 models: the spin-component-scaled MP2 for molecular interactions, SCS(MI)-MP2,[27] which empirically scales the MP2 contributions to obtain a more balanced treatment of intermolecular interactions, and Hesselman's MP2C,[28,29] which uses time-dependent density functional theory to improve the MP2 treatment of dispersion interactions.

The best of our calculations provide plausible energetics for the five oxalyl dihydrazide polymorphs that are consistent with the available experimental data and lie well within the usual 10 kJ/mol range for viable polymorphs. Crystal geometry, basis set, many-body polarization, three-body dispersion, and zero-point energy are all important to understanding oxalyl dihydrazide polymorphism. Contrary to the DFT-D results, we predict that the ε polymorph is actually slightly more stable than the α one at 0 K. This difference can largely be explained by the presence of three-body dispersion interactions in the HMBI model, which are missing from typical DFT-D approaches. Overall, these results suggest that empirical dispersion-corrected density functional methods should be used cautiously in molecular crystals.

2. THEORY

The hybrid many-body interaction model conceptually fragments a crystal into individual molecules.[26,30,31] The energetics of each molecule in the unit cell and its short-range pairwise interactions are computed quantum mechanically, while the long-range pairwise interactions and the many-body interactions are approximated using a polarizable force field whose parameters are calculated on the fly from QM calculations on each individual unit-cell molecule.

$$E^{\mathrm{HMBI}} = E^{\mathrm{QM}}_{\text{1-body}} + E^{\mathrm{QM}}_{\text{short-range 2-body}} + E^{\mathrm{MM}}_{\text{long-range 2-body}} + E^{\mathrm{MM}}_{\text{many-body}} \quad (1)$$

The partitioning of the two-body terms means that intermolecular interactions between pairs of molecules less than 9 Å are treated with QM, while interactions greater than 10 Å are treated with MM. Interactions between pairs of molecules separated by 9−10 Å are computed via interpolation between the QM and MM results, thereby ensuring smooth potential energy surfaces.

The *ab initio* force field (AIFF) used for the MM terms includes long-range two-body electrostatics, long-range self-consistent two-body induction, self-consistent many-body induction, and three-body Axilrod-Teller dispersion terms. The force field parameters (distributed multipole moments, distributed polarizabilities, and dispersion coefficients) are calculated from coupled Kohn−Sham theory for each molecule at its specific crystal geometry. In this sense, the model is almost entirely *ab initio*, though there are a few empirical damping functions that attenuate the induction and dispersion interactions at short-range. Additional details on the force-field model and the QM/MM partitioning are provided elsewhere.[26] See also related methods[32−43] and others described in two recent reviews.[25,44]

We have previously demonstrated that when high-level electronic structure methods are used for the QM parts, this model often predicts small-molecule crystal lattice energies to within experimental accuracy (1−2 kJ/mol)[26] and that it provides high-quality crystal structures that improve upon B3LYP-D* structures.[45] It has also provided useful insights into aspirin polymorphism[16] and calcium−uracil clusters.[46]

3. COMPUTATIONAL METHODS

First, we optimized the structures of the five polymorphs starting from the experimental structures (Cambridge Crystal Structure Database reference codes VIPKIO01−VIPKIO05).[21] In principle, one could optimize the experimental crystal structures with HMBI, but implementation of the HMBI gradients for the AIFF is ongoing. Instead, we optimized them using B3LYP-D* in the 6-31G(d,p) and TZP basis sets using CRYSTAL09.[47,48] The optimizations were started from the experimentally observed $P2_1/c$ space-group symmetry, and the gradients were converged to within 4.5×10^{-4} (MAX) and 3.0×10^{-4} (RMS) au, while the displacements were converged to within 1.8×10^{-4} (MAX) and 1.2×10^{-4} (RMS) au. The CRYSTAL09 two-electron integral tolerances were set to 10^{-7} (Coulomb overlap ITOL1), 10^{-7} (Coulomb penetration threshold ITOL2), 10^{-7} (HF exchange overlap ITOL3), 10^{-7} (HF exchange pseudo-overlap ITOL4), and 10^{-30} (HF exchange pseudo-overlap ITOL5), respectively.[48] A grid consisting of 55 radial points and up to 434 angular Lebedev points was used in evaluating the functional. A shrink factor of

Table 1. Optimized Lattice Parameters and Root-Mean-Square Deviations for the Five Polymorphs of Oxalyl Dihydrazide Compared to the Room-Temperature Experimental Structures

method	a (Å)	b (Å)	c (Å)	β (deg)	volume (Å^3)	rmsd$_{15}$[a] (Å)
			α polymorph			
experiment[b]	3.622	6.832	9.129	99.30	223.0	
B3LYP-D*/6-31G(d,p)	−3.66%	−1.24%	−1.44%	−1.81%	−5.80%	0.12
B3LYP-D*/TZP	−1.33%	−0.26%	−1.73%	−1.58%	−2.90%	0.09
D-PW91/pw[c]	−0.80%	−2.28%	−1.14%	−0.61%	−4.04%	0.10
			β polymorph			
experiment[b]	3.762	11.652	5.619	92.79	246.0	
B3LYP-D*/6-31G(d,p)	2.83%	−4.05%	−8.96%	−4.08%	−10.08%	0.41
B3LYP-D*/TZP	2.60%	−3.60%	−6.19%	−2.68%	−7.11%	0.30
D-PW91/pw[c]	7.95%	−6.39%	−8.84%	−1.19%	−7.81%	0.49
			γ polymorph			
experiment[b]	5.080	14.668	7.035	114.16	478.2	
B3LYP-D*/6-31G(d,p)	0.52%	−1.27%	−3.69%	2.42%	−6.58%	0.24
B3LYP-D*/TZP	0.55%	−0.88%	−1.43%	1.68%	−3.26%	0.14
D-PW91/pw[c]	−1.14%	−1.70%	0.00%	0.53%	−3.31%	0.12
			δ polymorph			
experiment[b]	3.661	14.550	5.065	119.01	235.9	
B3LYP-D*/6-31G(d,p)	4.26%	−3.15%	−0.05%	4.51%	−4.74%	0.32
B3LYP-D*/TZP	6.32%	−2.79%	0.05%	3.55%	−1.09%	0.31
D-PW91/pw[c]	1.86%	−3.90%	−0.89%	0.81%	−3.93%	0.18
			ε polymorph			
experiment[b]	5.364	3.841	12.319	109.00	240.0	
B3LYP-D*/6-31G(d,p)	2.52%	−4.91%	0.23%	3.19%	−4.52%	0.24
B3LYP-D*/TZP	3.86%	−3.56%	1.36%	3.76%	−1.25%	0.27
D-PW91/pw[c]	−0.39%	0.57%	−1.44%	3.01%	−3.43%	0.19

[a]Root-mean-square deviation of atomic positions, excluding hydrogen atoms. [b]Ref 21. [c]Planewave D-PW91 structures from ref 20.

eight for the reciprocal lattice vectors was used, leading to 170 points in the irreducible Brillouin zone. For comparison, we also obtained the D-PW91/planewave basis geometries from ref 20. Structural analysis, including root-mean-square deviations (rmsd$_{15}$ values)[49] on all three sets of structures was performed using Mercury 3.0[50]

Single-point, counterpoise-corrected energies were then computed on each of these three sets of structures using a variety of methods. Single-point periodic B3LYP-D* energies were computed on each set of geometries in CRYSTAL09 using at least 200 ghost atoms surrounding a central molecule. We also performed a series of HMBI single-point energy calculations on each set of structures.

When using the HMBI model, the user must choose a model chemistry for the QM terms, a basis set to use when calculating the AIFF parameters, and at what distance to transition from a quantum to classical treatment of the pairwise interactions. In this work, we use a consistent set of AIFF parameters for all cases. Specifically, we used the triple-ζ Sadlej basis[51] and the procedures described previously[26,52] to compute the AIFF parameters using the Camcasp[53] software package. A vertical ionization potential of 0.3701 hartree was computed for oxalyl dihydrazide at the B3LYP/6-311++G(3df,2p) level and is used in the asymptotic correction during the force field property calculations. Evaluation of the force field used conservative cutoffs for induction (25 Å), two-body dispersion (25 Å), and three-body dispersion (15 Å). The Ewald summation was also converged to within 10^{-3} kJ/mol or better. See ref 26 for details of the force field model.

The QM terms were evaluated with several different electronic structure methods. First, we used counterpoise-corrected dual-basis RI-MP2[54] with the aug-cc-pVXZ (X = D,T,Q) basis sets[55−57] and extrapolated to the complete basis set limit using a standard two-point TQ extrapolation.[58,59] Second, to obtain SCS(MI) RI-MP2 data, we rescaled the RI-MP2 correlation energies for each monomer and dimer with the appropriate spin-component-scaling parameters.[27] All of these calculations were performed with a development version of Q-Chem.[60] Third, we computed an MP2C dispersion correction[28,29] for each pairwise intermolecular interaction in the aug-cc-pVTZ basis with Molpro[61] and used this correction with the RI-MP2 data to estimate the complete-basis-set MP2C results for the crystals. As noted in previous benchmark studies,[29] the MP2C dispersion correction is only moderately sensitive to the basis set. In oxalyl dihydrazide, we obtained similar MP2C results with the smaller aug-cc-pVDZ basis, suggesting that aug-cc-pVTZ is sufficiently large here. Unless otherwise explicitly stated, all HMBI energies reported below are estimated complete-basis-set extrapolated values.

4. RESULTS AND DISCUSSION

4.1. Crystal Structure Optimization. The experimental crystal structures for all five polymorphs were optimized using B3LYP-D* in both the 6-31G(d,p) and TZP basis sets. Table 1 compares the resulting lattice parameters to the experimental[21] and previously published D-PW91 ones.[20] The structures determined with the TZP basis are fairly accurate, with most lattice parameters predicted to within a few percent of these experimental values. The volumes of all five crystals are underestimated, which fits with the thermal expansion of the crystal structure one expects between 0 K (computed) and room temperature (experiments). Unsurprisingly, the largest errors occur for the β polymorph, which was difficult to

produce experimentally and consequently has much larger uncertainties in its experimental structure.[21]

The D-PW91/pw structures differ moderately from those determined here at the B3LYP-D*/TZP level. The D-PW91 errors in the individual lattice parameters are often smaller, but the B3LYP-D*/TZP volumes tend to be closer to experimental values. Overall, both functionals/basis sets produce crystal structures that lie within the few percent errors expected due to thermal expansion,[62] making it difficult to say for certain which set of structures is superior. The root-mean-square deviations ($rmsd_{15}$) values for the atomic positions are also fairly comparable. The B3LYP-D*/TZP value is notably better for the β polymorph, though it is somewhat worse for the δ and ε ones.

The planewave basis set used in the D-PW91 calculations avoids basis set superposition error (BSSE), which can be significant here. On the other hand, the B3LYP-D* structures appear to be closer to the MP2 optimized structures, as discussed below. For these reasons and to help assess the convergence of our predictions, we perform higher-level single-point energy calculations on all three sets of structures, as described in the next section.

4.2. High-Level HMBI Results. We begin by examining the relative energies at the HMBI MP2 level on the B3LYP-D*/TZP structures, as shown in Figure 2. The energy of the α polymorph relative to the other four forms is very sensitive to the basis set. The qualitative MP2 polymorph ordering does not converge until the aug-cc-pVQZ basis, and significant quantitative changes occur even in the complete-basis-set extrapolation.

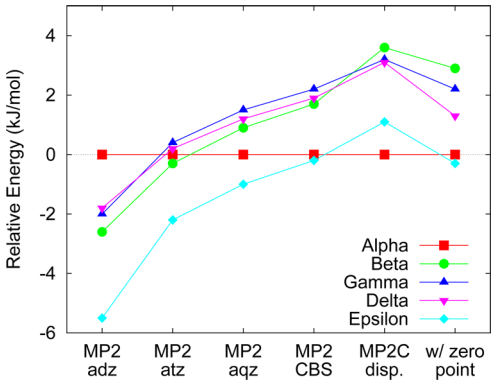

Figure 2. HMBI-predicted polymorph energies using the B3LYP-D*/TZP geometries. The figure shows basis-set convergence at the RI-MP2 level, the impact of the MP2C dispersion correction, and the zero-point energy contributions. Experiments suggest α, δ, $\varepsilon < \gamma < \beta$.

This behavior contrasts markedly from our earlier work on aspirin, where the energy difference between the two polymorphs is well-converged even with a double-ζ basis set.[16] In aspirin, however, the two crystal packing motifs are very similar, so the polymorph energy difference benefits tremendously from error cancellation. In oxalyl dihydrazide, the severe basis-set dependence results from a BSSE that does not cancel well between polymorphs. Specifically, the oxalyl dihydrazide α polymorph exhibits purely intermolecular hydrogen bonding, while the other four forms involve some intramolecular hydrogen bonding. The intermolecular BSSE is approximately corrected by applying the standard counterpoise correction to each dimer interaction in HMBI, but this does not correct the intramolecular BSSE. Therefore, the polymorphs with intramolecular hydrogen bonding interactions (β, γ, δ, and ε) are artificially stabilized relative to the α form in incomplete basis sets. As the basis set approaches completeness, this intramolecular BSSE resolves itself, and the α polymorph ends up being one of the most stable polymorphs. Unfortunately, this strong dependence on basis set in oxalyl dihydrazide may be typical behavior for conformational polymorphs distinguished by significantly different packing, since the aspirin-like error cancellation will not occur.

The resulting HMBI MP2/CBS-limit energies have almost the right stability order, except that the γ polymorph is slightly less stable than the β one. However, the delocalized π electrons on the oxalyl dihydrazide backbone interact with neighboring molecules through π-type dispersion interactions, and it is well-known that MP2 often overestimates such interactions. Therefore, we employed two different schemes for correcting this overestimation: MP2C and SCS(MI) MP2.

Though SCS(MI) MP2 often performs very well for noncovalent interactions, it behaves poorly here. As shown in Figure 3, the energetic ordering is wrong, with the α polymorph being much too high in energy. The other four polymorph energies are reasonable relative to one another. Optimal spin-component scaling factors for intra- and intermolecular interactions are nearly opposite,[27,63−65] so the subtle balances here between intermolecular and intramolecular interactions (including both pyramidalization of the nitrogens and the intramolecular hydrogen bonding) may be too challenging for spin-component-scaled MP2.

In contrast, the MP2C method, which uses time-dependent DFT to improve upon the uncoupled Hartree−Fock treatment of dispersion in conventional MP2, performs much better. The MP2C method corrects only the pairwise intermolecular interactions, but the problematic π-type dispersion interactions in oxalyl dihydrazide are indeed intermolecular. As expected, the MP2C crystal binding energies that result from correcting each QM pairwise interaction energy are 2−3% (3−5 kJ/mol) smaller than the MP2 ones, and it improves the relative polymorph ordering. It destabilizes all four other polymorphs relative to the α one, making α the most stable form. The β form undergoes the largest shift and becomes the least stable polymorph, as expected from experiments. The β form exhibits the closest intermolecular π-stacking distance of any of the polymorphs (3.2 Å) and has the strongest π-stacking interactions at the MP2 level, so it is unsurprising that the MP2C correction is largest for that polymorph.

Finally, we add in zero-point energy contributions which were computed from harmonic vibrational frequencies computed at the Γ point with B3LYP-D*/6-31G(d,p). The harmonic frequencies were not scaled, but scaling would only trivially affect the small relative zero-point contributions found here. Overall, zero-point energy stabilizes the β, γ, δ, and ε polymorphs by 1−2 kJ/mol relative to the α form. The stronger intermolecular hydrogen bonds in the α polymorph lead to a larger zero-point energy, which destabilizes that polymorph.

The final MP2C results appear very plausible with regard to experimental results. Bear in mind, of course, that the experimental ordering was determined at finite temperatures, while these predictions are at 0 K and neglect thermal/entropic effects. From our best predictions, $\varepsilon < \alpha < \delta < \gamma < \beta$ at 0 K, though the ε polymorph is only slightly more stable than the α one. According to the density rule, one might expect the dense α polymorph to be the most stable. However, the density rule is

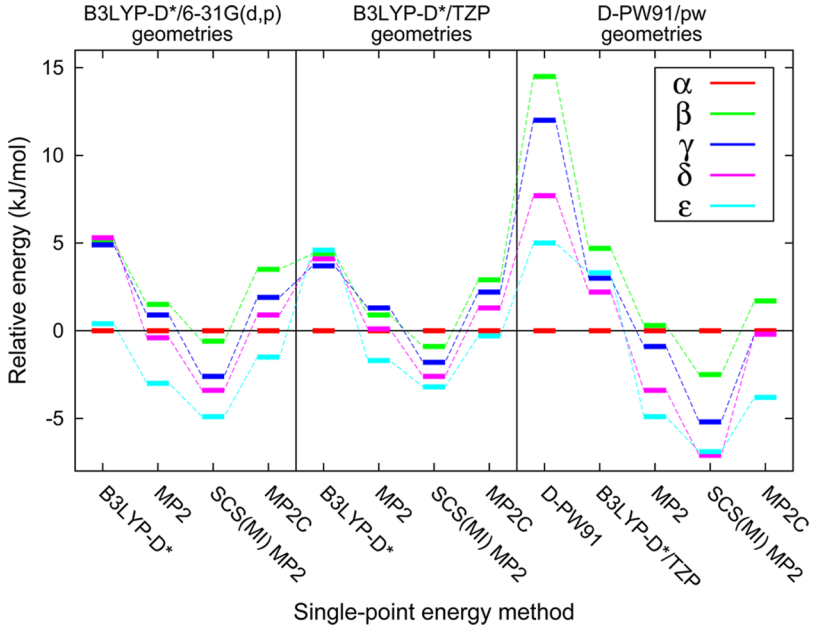

Figure 3. Comparison of relative polymorph single-point energy predictions from different electronic structure methods and different optimized crystal geometries. All energies include a B3LYP-D*/6-31G(d,p) harmonic zero-point contribution. Experiments suggest α, δ, $\varepsilon < \gamma < \beta$. MP2C obtains a plausible ordering for both B3LYP-D* geometries.

based on maximizing the nonspecific van der Waals interactions. Exceptions to this rule are common when intermolecular hydrogen bonding is important, as in oxalyl dihydrazide.[66]

Significantly, the same qualitative ordering and similar energetics are obtained regardless of whether one uses the B3LYP-D*/TZP or 6-31G(d,p) structures (Figure 3), bolstering confidence in these predictions. In both cases, the overall energy range of the five polymorphs spans ~5 kJ/mol. In fact, all of the MP2-level results place the five polymorphs within a range well below 10 kJ/mol, as should typically be expected. These results are in marked contrast from the ~15 kJ/mol range for the D-PW91 energies.[20]

4.3. Comparison with Density Functional Methods. To understand the discrepancies between the HMBI and D-PW91 results better, we (1) examine the B3LYP-D* relative energies on the B3LYP-D* structures and (2) compute a variety of single-point energies on the D-PW91 structures from ref 20. As noted previously,[20] B3LYP gives very poor energetics in the absence of a dispersion correction, with the α polymorph the least stable polymorph and an overall polymorph energy range of 10−15 kJ/mol.

The dispersion-corrected B3LYP-D* polymorph energies behave better, though they differ dramatically from those predicted by D-PW91, as shown in Figure 3. Whereas the D-PW91 structures predict an overly broad energy range for the five polymorphs, the B3LYP-D* energy ranges are qualitatively similar to those from the MP2-level HMBI calculations. This effect is not merely due to the differences in the structures, either. Single-point B3LYP-D*/TZP energetics on the D-PW91 structures are similar to those on the B3LYP-D* structures, and they are very different from the D-PW91 energetics.

However, the specific B3LYP-D* polymorph ordering is inconsistent with existing experimental data. Interestingly, all of the DFT-D calculations agree that the α polymorph is the most stable, contrary to what MP2C predicts for either set of the B3LYP-D*-optimized structures. This point will be revisited in section 4.4. In any case, these two widely used dispersion-corrected density functionals for molecular crystals make very different and experimentally unsatisfactory predictions, calling into question their reliability in oxalyl dihydrazide.

To help decouple the effects between optimized structure and energetics, we performed a series of single-point HMBI calculations on the D-PW91 structures. The MP2, SCS(MI) MP2, and MP2C energies computed for these structures exhibit a major difference from the results obtained using the same methods on the B3LYP-D* structures. All three MP2-type methods predict a reasonable order for the β, γ, δ, and ε forms with the D-PW91 structures, but they are overstabilized relative to the α polymorph. The same relative destabilization of the α polymorph also plagued the SCS(MI) MP2 results discussed in section 4.2. Clearly, the differences in intra- and intermolecular interactions between the α and other polymorphs provide the key challenge in predicting a proper oxalyl dihydrazide polymorph ordering.

Examination of the total MP2C crystal energies (Table 2) provides insight. Whereas the total MP2C single-point energies

Table 2. Comparison of Single-Point Estimated HMBI MP2C/CBS-Limit Energies of the Different Optimized Structures[a]

	geometry optimization method:		
polymorph	B3LYP-D*/TZP (hartrees)	B3LYP-D*/6-31G(d,p) (kJ/mol)	D-PW91 (kJ/mol)
α	−448.787206	0.3	4.3
β	−448.785826	1.0	3.1
γ	−448.786002	0.0	1.9
δ	−448.786012	−0.1	0.9
ε	−448.786792	−0.9	0.9

[a]The absolute energies per molecule are given for the B3LYP-D*/TZP structures, while the other structures are presented relative to the B3LYP-D*/TZP structure values in kJ/mol per molecule.

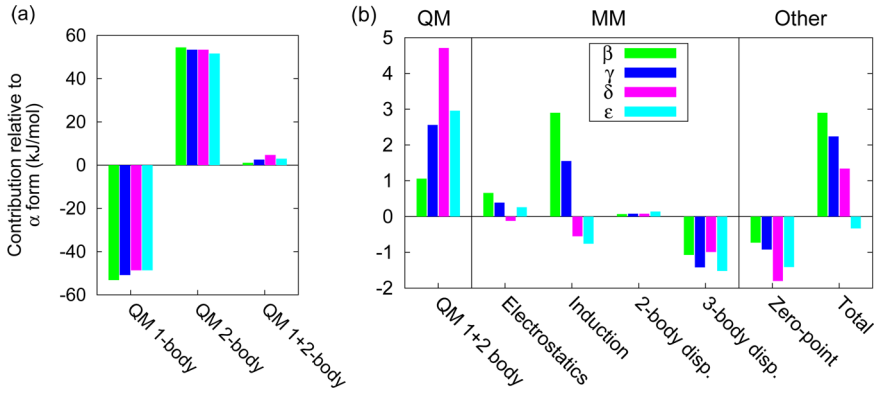

Figure 4. Decomposition of the best HMBI MP2C energies on the B3LYP-D*/TZP geometries. (a) Comparison of the intra- and intermolecular QM contributions and (b) comparison of the total QM contributions with the force-field and zero-point ones, all in kilojoules per mole per molecule relative to the α polymorph. A negative value for β, γ, δ, or ε indicates that the interaction is more favorable than in the α polymorph, while a positive value means the interaction in the α polymorph is preferred.

for both B3LYP-D* geometries lie within 1.0 kJ/mol of each other, the MP2C single-point energies on the D-PW91 structures are up to 4 kJ/mol higher. In other words, all of the D-PW91 geometries are somewhat further from the optimal MP2C structures than B3LYP ones. Because this energy difference is most extreme for the α polymorph, it is destabilized relative to the other forms.

Energetic decomposition of the HMBI MP2C energies along the lines used in section 4.4 below and comparison of the experimental, B3LYP-D*, and D-PW91 structures indicates that the α polymorph destabilization for the D-PW91 structures arises from an intramolecular dihedral rotation of the terminal oxalyl dihydrazide amine groups away from the experimental angle. According to the HMBI MP2C results, this intramolecular distortion improves the intermolecular interactions and many-body induction (e.g., better intermolecular hydrogen bonding) by about 10 kJ/mol per molecule, but the 14 kJ/mol intramolecular energy penalty outweighs the improved intermolecular interactions. In contrast, the lower-energy B3LYP-D* α form terminal amine groups align more closely with the experimental structures.

We have previously demonstrated that HMBI MP2-optimized crystal structures give excellent agreement (better than DFT-D) with low-temperature experimental structures in a test set of five small crystals.[45] So, while MP2-quality geometries are not available here, the MP2C single-point energy data indicate that the B3LYP-D* structures are energetically superior to the D-PW91 values.

4.4. Energy Decomposition. Another powerful feature of the HMBI fragment method is the ability to decompose the energetic contributions into intramolecular (QM 1-body); short-range pairwise intermolecular (QM 2-body); and the electrostatic, induction, and dispersion force-field terms describing long-range and many-body interactions. Figure 4 shows the relative energy contributions for the various interactions relative to the α polymorph.

As shown in Figure 4a, the intramolecular (QM 1-body) terms favor forms β, γ, δ, and ε by roughly 50 kJ/mol per molecule due to the two intramolecular hydrogen bonds found in each molecule in those structures. The β polymorph, which is overall the least stable, adopts the most favorable intramolecular structure. On the other hand, the α form is favored by about 50 kJ/mol in the short-range intermolecular (QM 2-body) terms because of its strong intermolecular hydrogen bonding. As noted previously, the α polymorph is the only one that forms two "geometrically optimal" hydrogen bonds with each terminal amine group.[20] Upon combining both sets of contributions, the purely intermolecular hydrogen bonding in the α polymorph is preferred by 1−5 kJ/mol according to MP2C. Of course, this balance is sensitive to the crystal geometry and electronic structure method, as discussed above.

As shown in Figure 4b, the induction contribution (combining long-range two-body and many-body contributions) and Axilrod-Teller three-body dispersion also make large relative contributions. Induction further destabilizes the β and γ polymorphs relative to the α, δ, and ε ones. In other words, the three most stable polymorphs all benefit from strong many-body intermolecular induction effects.

Analysis of the crystal structures indicates that the δ and ε polymorphs form chains of hydrogen bonds aligned along a single direction, leading to strong many-body induction effects. The α polymorph two-dimensional hydrogen-bond chains are also somewhat directional, while in the β polymorph they are oriented in many different directions in three-dimensions, reducing the overall many-body induction contribution. In the γ polymorph, the hydrogen bonding occurs in dimers, rather than forming infinite chains, which reduces its many-body induction contribution.

The intermolecular three-body dispersion is actually less repulsive for every polymorph other than α, so it compresses the energy spacing between the other four forms and the α form by about 1−1.5 kJ/mol. This can be understood from the higher density of the α form (1.76 g/cm^3) compared to the other forms, (1.59−1.66 g/cm^3). Finally, all four polymorphs are stabilized relative to α by zero-point energy. The α form exhibits the strongest intermolecular interactions, leading to larger vibrational frequencies and a bigger zero-point contribution than in the other structures.

As noted in section 4.3, the DFT calculations predict that the α polymorph is the most stable, while all of the HMBI MP2-level calculations predict that the ε form is more stable. A large portion of this difference comes from the three-body dispersion contribution in HMBI. As shown in Figure 5, the inclusion of three-body dispersion reverses the stability order of the α and ε polymorphs. Three-body dispersion is not included in typical empirical DFT dispersion corrections (they only include two-body contributions), and attempting to add three-body

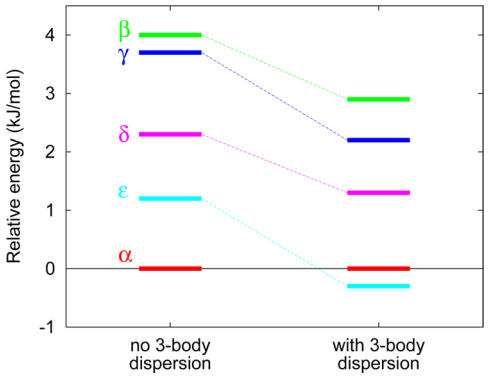

Figure 5. Three-body dispersion slightly compresses the energy differences between polymorphs and reverses the stability of the α and ε polymorphs. Based on the HMBI MP2C energies with the B3LYP-D*/TZP geometries.

dispersion corrections to DFT can be problematic,[67] though promising new methods are appearing.[9]

Experimentally, it is unclear whether the α or ε polymorph is more stable. As noted above, the density rule would suggest that the more dense α polymorph is the most stable, but exceptions for hydrogen-bonded crystals like oxalyl dihydrazide are common. So the HMBI MP2-level orderings are plausible. Given that we have previously demonstrated that the HMBI three-body dispersion contributions are fairly reliable compared to more elaborate dispersion models,[25,26] these results appear reasonable and provide further evidence for the importance of including three-body dispersion in molecular crystal studies.[25,26,36,68]

5. CONCLUSIONS

Quantum mechanical calculations are rapidly becoming routine in molecular crystal structure modeling, bringing us substantially closer to the dream of first-principles crystal structure prediction. However, cases such as oxalyl dihydrazide, which has five known conformational polymorphs separated by small energy gaps, highlight the difficulties of crystal polymorph prediction. Obtaining reliable energetics in oxalyl dihydrazide requires a careful balance between inter- and intramolecular interactions, many-body induction, three-body dispersion effects, and zero-point energies, making it a stringent test for molecular crystal models. The primary challenge lies in determining the relative energy differences between the intermolecularly hydrogen bonded α polymorph and the other four polymorphs, which mix inter- and intramolecular hydrogen bonds.

Although empirical dispersion-corrected density functionals can perform well for polymorph prediction, they appear to struggle in challenging systems such as oxalyl dihydrazide or aspirin.[16] Here, we demonstrated that two different DFT-D methods make very different predictions in oxalyl dihydrazide, neither of which agrees satisfactorily with higher-level calculations and experimental results. While the comparison with experimental results is clouded by the different conditions (e.g., calculations at 0 K versus experiments at finite temperatures) and incomplete experimental data, the fact that two seemingly reasonable empirical DFT-D functionals do not even qualitatively agree with each other or with higher-level calculations raises troubling questions about their reliability for challenging polymorphic molecular crystals. In the future, it would be interesting to compare how newer nonempirical dispersion corrections for DFT perform in this challenging system.

Fragment methods promise to bring the full predictive power of high-level quantum chemistry techniques to molecular crystal modeling with relatively low computational cost, making it feasible to handle the subtle energetic balances, assuming accurate enough electronic structure methods are employed. In the case of oxalyl dihydrazide, neither MP2 nor SCS(MI) MP2 quite manages to balance the forces correctly, but MP2C appears to do so when it is combined with very large-basis MP2 results and a treatment of many-body and zero-point effects. Clearly, the long-standing search for accurate, low-cost electronic structure methods capable of describing the full range of intra- and intermolecular interactions remains as important as ever.

■ ASSOCIATED CONTENT

Supporting Information

Optimized crystal structure CIF files, single-point energies, and lattice energies are provided. This material is available free of charge via the Internet at http://pubs.acs.org.

■ AUTHOR INFORMATION

Corresponding Author

*E-mail: gregory.beran@ucr.edu.

Notes

The authors declare no competing financial interest.

■ ACKNOWLEDGMENTS

Funding for this work from the National Science Foundation (CHE-1112568) and supercomputer time from the Teragrid (TG-CHE110064) are gratefully acknowledged. We thank Dr. John Kendrick for providing the D-PW91 optimized structures used in their earlier study on oxalyl dihydrazide.

■ REFERENCES

(1) Price, S. L. *Int. Rev. Phys. Chem.* **2008**, *27*, 541−568.
(2) Kazantsev, A. V.; Karamertzanis, P. G.; Adjiman, C. S.; Pantelides, C. C. *J. Chem. Theory Comput.* **2011**, *7*, 1998−2016.
(3) Lu, D.; Li, Y.; Rocca, D.; Galli, G. *Phys. Rev. Lett.* **2009**, *102*, 206411.
(4) Li, Y.; Lu, D.; Nguyen, H.-V.; Galli, G. *J. Phys. Chem. A* **2010**, *114*, 1944−1952.
(5) Marom, N.; Tkatchenko, A.; Kapishnikov, S.; Kronik, L.; Leiserowitz, L. *Cryst. Growth Des.* **2011**, *11*, 3332−3341.
(6) Pedone, A.; Presti, D.; Menziani, M. C. *Chem. Phys. Lett.* **2012**, *541*, 12−15.
(7) Schatschneider, B.; Liang, J.-J.; Jezowski, S.; Tkatchenko, A. *CrystEngComm* **2012**, *14*, 4656−4663.
(8) Wu, J.; Gygi, F. *J. Chem. Phys.* **2012**, *136*, 224107.
(9) Tkatchenko, A.; DiStasio, R. A.; Car, R.; Scheffler, M. *Phys. Rev. Lett.* **2012**, *108*, 236402.
(10) Grimme, S. *WIRES: Comput. Mol. Sci.* **2011**, *1*, 211−228.
(11) Neumann, M. A.; Leusen, F. J. J.; Kendrick, J. *Angew. Chem., Int. Ed.* **2008**, *47*, 2427−2430.
(12) Day, G. M.; et al. *Acta Cryst. B* **2009**, *65*, 107−25.
(13) Bardwell, D. A.; et al. *Acta Cryst. B* **2011**, *67*, 535−51.
(14) Kendrick, J.; Leusen, F. J. J.; Neumann, M. A.; van de Streek, J. *Chem.—Eur. J.* **2011**, *17*, 10736−10744.
(15) Kazantsev, A. V.; Karamertzanis, P. G.; Adjiman, C. S.; Pantelides, C. C.; Price, S. L.; Galek, P. T. A.; Day, G. M.; Cruz-Cabeza, A. J. *Int. J. Pharm.* **2011**, *418*, 168−178.
(16) Wen, S.; Beran, G. J. O. *Cryst. Growth Des.* **2012**, *12*, 2169−2172.

(17) Hongo, K.; Watson, M. A.; Sanchez-Carrera, R. S.; Iitaka, T.; Aspuru-Guzik, A. *J. Phys. Chem. Lett.* **2010**, *1*, 1789−1794.
(18) Freeman, C. M.; Andzelm, J. W.; Ewig, C. S.; Hill, J.-R.; Delley, B. *Chem. Commun.* **1998**, 2455−2456.
(19) Rivera, S. A.; Allis, D. G.; Hudson, B. S. *Cryst. Growth. Des.* **2008**, *8*, 3905−3907.
(20) Karamertzanis, P. G.; Day, G. M.; Welch, G. W. a.; Kendrick, J.; Leusen, F. J. J.; Neumann, M. a.; Price, S. L. *J. Chem. Phys.* **2008**, *128*, 244708.
(21) Ahn, S.; Guo, F.; Kariuki, B. M.; Harris, K. D. M. *J. Am. Chem. Soc.* **2006**, *128*, 8441−52.
(22) Bernstein, J. *Polymorphism in Molecular Crystals*; Clarendon Press: Oxford, 2002; pp 154−155.
(23) Civalleri, B.; Zicovich-Wilson, C. M.; Valenzano, L.; Ugliengo, P. *CrystEngComm* **2008**, *10*, 405−410.
(24) Pisani, C.; Schütz, M.; Casassa, S.; Usvyat, D.; Maschio, L.; Lorenz, M.; Erba, A. *Phys. Chem. Chem. Phys.* **2012**, *14*, 7615−7628.
(25) Wen, S.; Nanda, K.; Huang, Y.; Beran, G. J. O. *Phys. Chem. Chem. Phys.* **2012**, *14*, 7578−7590.
(26) Wen, S.; Beran, G. J. O. *J. Chem. Theory Comput.* **2011**, *7*, 3733−3742.
(27) Distasio, R. A.; Head-Gordon, M. *Mol. Phys.* **2007**, *105*, 1073−1083.
(28) Hesselmann, A. *J. Chem. Phys.* **2008**, *128*, 144112.
(29) Pitonak, M.; Hesselmann, A. *J. Chem. Theory Comput.* **2010**, *6*, 168−178.
(30) Beran, G. J. O. *J. Chem. Phys.* **2009**, *130*, 164115.
(31) Beran, G. J. O.; Nanda, K. *J. Phys. Chem. Lett.* **2010**, *1*, 3480−3487.
(32) Nagayoshi, K.; Ikeda, T.; Kitaura, K.; Nagase, S. *J. Theory. Comput. Chem.* **2003**, *2*, 233−244.
(33) Dahlke, E. E.; Truhlar, D. G. *J. Chem. Theory Comput.* **2007**, *3*, 1342−1348.
(34) Hermann, A.; Schwerdtfeger, P. *Phys. Rev. Lett.* **2008**, *101*, 183005.
(35) Bludsky, O.; Rubes, M.; Soldan, P. *Phys. Rev. B* **2008**, *77*, 092103.
(36) Podeszwa, R.; Rice, B. M.; Szalewicz, K. *Phys. Rev. Lett.* **2008**, *101*, 115503.
(37) Hirata, S. *J. Chem. Phys.* **2008**, *129*, 204104.
(38) Sode, O.; Keceli, M.; Hirata, S.; Yagi, K. *Int. J. Quantum Chem.* **2009**, *109*, 1928−1939.
(39) Addicoat, M.; Collins, M. A. *J. Chem. Phys.* **2009**, *131*, 104103.
(40) Neill, D. P. O.; Allan, N. L.; Manby, F. R. Ab initio Monte Carlo simulations of liquid water. In *Accurate Quantum Chemistry in the Condensed Phase*; Manby, F., Ed.; CRC Press, 2010; pp 163−193.
(41) Tsuzuki, S.; Orita, H.; Honda, K.; Mikami, M. *J. Phys. Chem. B* **2010**, *114*, 6799−6805.
(42) Taylor, C. R.; Bygrave, P. J.; Hart, J. N.; Allan, N. L.; Manby, F. R. *Phys. Chem. Chem. Phys.* **2012**, *14*, 7739−7743.
(43) Müller, C.; Paulus, B. *Phys. Chem. Chem. Phys.* **2012**, *14*, 7605−7614.
(44) Gordon, M. S.; Fedorov, D. G.; Pruitt, S. R.; Slipchenko, L. *Chem. Rev.* **2011**, *112*, 632−672.
(45) Nanda, K.; Beran, G. J. O. *J. Chem. Phys.* **2012**, submitted.
(46) Gillis, E. A. L.; Demireva, M.; Nanda, K.; Beran, G. J. O.; Williams, E. R.; Fridgen, T. D. *Phys. Chem. Chem. Phys.* **2012**, *14*, 3304−3315.
(47) Dovesi, R.; Orlando, R.; Civalleri, B.; Roetti, C.; Saunders, V. R.; Zicovich-Wilson, C. M. *Z. Kristallogr.* **2005**, *220*, 571−573.
(48) Dovesi, R.; Saunders, V. R.; Roetti, C.; Orlando, R.; Zicovich-Wilson, C. M.; Pascale, F.; Civalleri, B.; Doll, K.; Harrison, N. M.; Bush, I. J.; D'Arco, P.; Llunell, M.; Science, C.; Technologies, A. *CRYSTAL09 User's Manual*; University of Torino: Torino, 2009.
(49) Chisholm, J. A.; Motherwell, W. D. S. *J. Appl. Crystallogr.* **2005**, *38*, 228−231.
(50) Macrae, C. F.; Bruno, I. J.; Chisholm, J. A.; Edgington, P. R.; McCabe, P.; Pidcock, E.; Rodriguez-Monge, L.; Taylor, R.; van de Streek, J.; Wood, P. A. *J. Appl. Crystallogr.* **2008**, *41*, 455−470.
(51) Sadlej, A. J. *Collect. Czech. Chem. Commun.* **1988**, *53*, 1995−2016.
(52) Sebetci, A.; Beran, G. J. O. *J. Chem. Theory Comput.* **2010**, *6*, 155−167.
(53) Misquitta, A. J.; Stone, A. J.; , CamCASP v5.6 (2011), http://www-stone.ch.cam.ac.uk/programs.html. Accessed Februrary 23, 2011.
(54) Steele, R. P.; Distasio, R. A.; Shao, Y.; Kong, J.; Head-Gordon, M. *J. Chem. Phys.* **2006**, *125*, 074108.
(55) Dunning, T. H. *J. Chem. Phys.* **1989**, *90*, 1007−1023.
(56) Weigend, F.; Köhn, A.; Hättig, C. *J. Chem. Phys.* **2002**, *116*, 3175−3183.
(57) Steele, R. P.; Distasio, R. A.; Head-Gordon, M. *J. Chem. Theory Comput.*. **2009**, *5*, 1560−1572.
(58) Karton, A.; Martin, J. M. L. *Theor. Chem. Acc.* **2006**, *115*, 330−333.
(59) Helgaker, T.; Klopper, W.; Koch, H.; Noga, J. *J. Chem. Phys.* **1997**, *106*, 9639−9646.
(60) Shao, Y.; et al. *Phys. Chem. Chem. Phys.* **2006**, *8*, 3172−3191.
(61) MOLPRO, version 2010.1, a package of ab initio programs, H.-J.Werner, Knowles, P. J.; Knizia, G.; Manby, F. R.; M. Schütz, Celani, P.; Korona, T.; Lindh, R.; Mitrushenkov, A.; Rauhut, G.; Shamasundar, K. R.; Adler, T. B.; Amos, R. D.; Bernhardsson, A.; Berning, A.; Cooper, D. L.; Deegan, M. J. O.; Dobbyn, A. J.; Eckert, F.; Goll, E.; Hampel, C.; Hesselmann, A.; Hetzer, G.; Hrenar, T.; Jansen, G.; C. Köppel, Liu, Y.; Lloyd, A. W.; Mata, R. A.; May, A. J.; Mchnicholas, S. J.; Meyer, W.; Mura, M. E.; Nicklass, A.; D. P. O'Neill, Palmieri, P.; K. Pflüger, Pitzer, R.; Reiher, M.; Shiozaki, T.; Stoll, H.; Stone, A. J.; Tarroni, R.; Thorsteinsson, T.; Wang, M.; , Wolf, A.; . See http://www.molpro.net.
(62) Beyer, T.; Price, S. L. *CrystEngComm* **2000**, *2*, 183.
(63) Gerenkamp, M.; Grimme, S. *Chem. Phys. Lett.* **2004**, *392*, 229−235.
(64) Takatani, T.; Hohenstein, E. G.; Sherrill, C. D. *J. Chem. Phys.* **2010**, *128*, 124111.
(65) Pitonak, M.; Rezac, J.; Hobza, P. *Phys. Chem. Chem. Phys.* **2010**, *12*, 9611−9614.
(66) Bernstein, J. *Polymorphism in Molecular Crystals*; Clarendon Press: Oxford, 2002; pp 40−41.
(67) Tkatchenko, A.; von Lilienfeld, O. *Phys. Rev. B* **2008**, *78*, 045116.
(68) von Lilienfeld, O. A.; Tkatchenko, A. *J. Chem. Phys.* **2010**, *132*, 234109.